Electronic Supplementary Material (ESI) for Dalton Transactions.

Supporting information

The synthesis and magnetic properties of a linear mixed-valence $[Ni_3]^{5+}$ in anthyridine tri-nickel complex

Chang-Lin Hsieh[a], Tsai-Jung Liu[a], You Song[b], Gene-Hsiang Lee[a] ,Bih-Yaw Jin[a], Tien-Sung Lin[a] and Shie-Ming Peng[a,c*]

[a] Department of Chemistry, National Taiwan University

[b] State Key Laboratory of Coordinate Chemistry, School of Chemistry and Chemical Engineering, Nanjing Nantional Laboratory of Microstructures, Nanjing University, P. R. China.

[c] Institute of Chemistry, Academia Sinica

Corresponding author E-mail : smpeng@ntu.edu.tw

Synthesis of $[Ni_3(dbay)_4Cl_2]I_3$

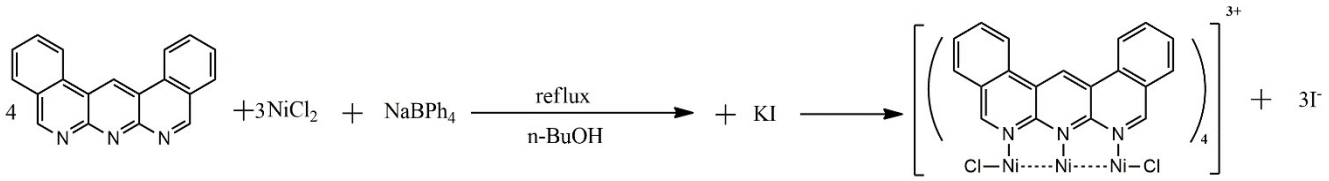

Synthesis of $[Ni_3(dbay)_4Cl_2]I_3$. The 1,13,14-Tetra-dibenz[*a,j*]anthracene (0.20 g, 0.071 mol), $NiCl_2$ (0.1 g, 0.058 mol), $NaB(C_6H_5)_4$ (0.22 g, 0.065 mol), and 10 mL n-BuOH were placed in a 25 mL round bottom flask. The mixure was then heated to ~150 °C and kept at the temperature for 48 hrs. The solvent was removed under reduce pressure. The dark red crystal was obtained with KI from diffusion of ether into DMF solution. Yield: 24 mg 10%.

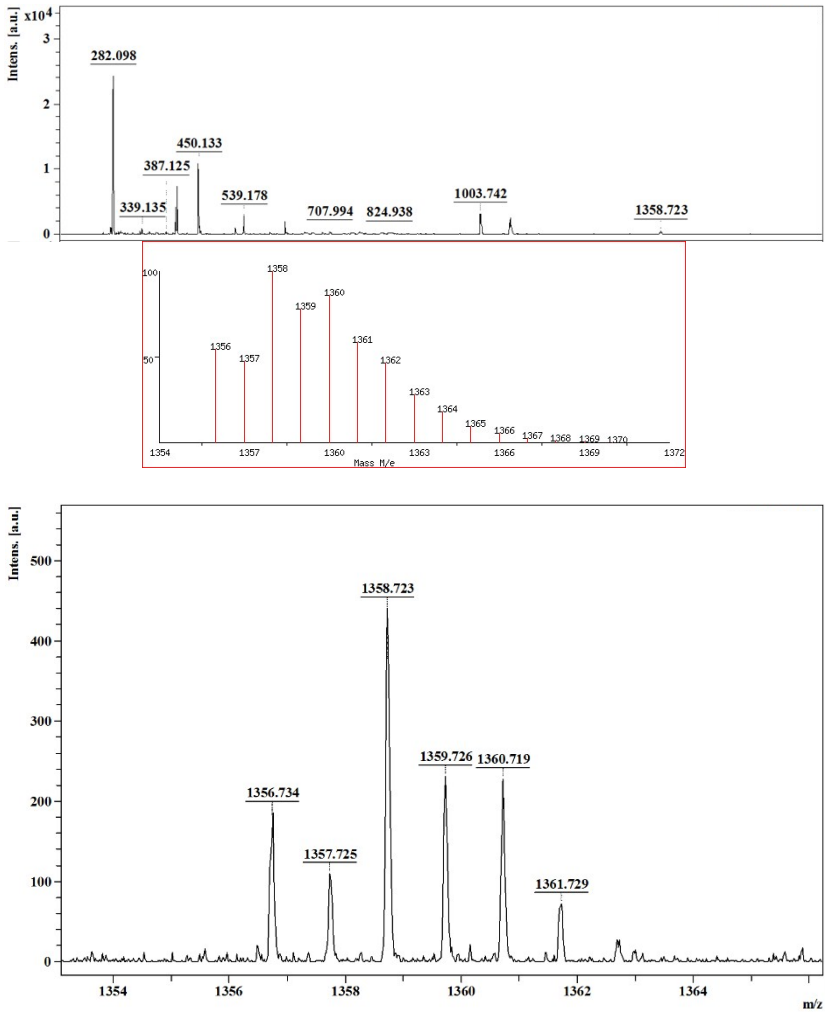

Figure. S1 MALDI mass spectra of 1

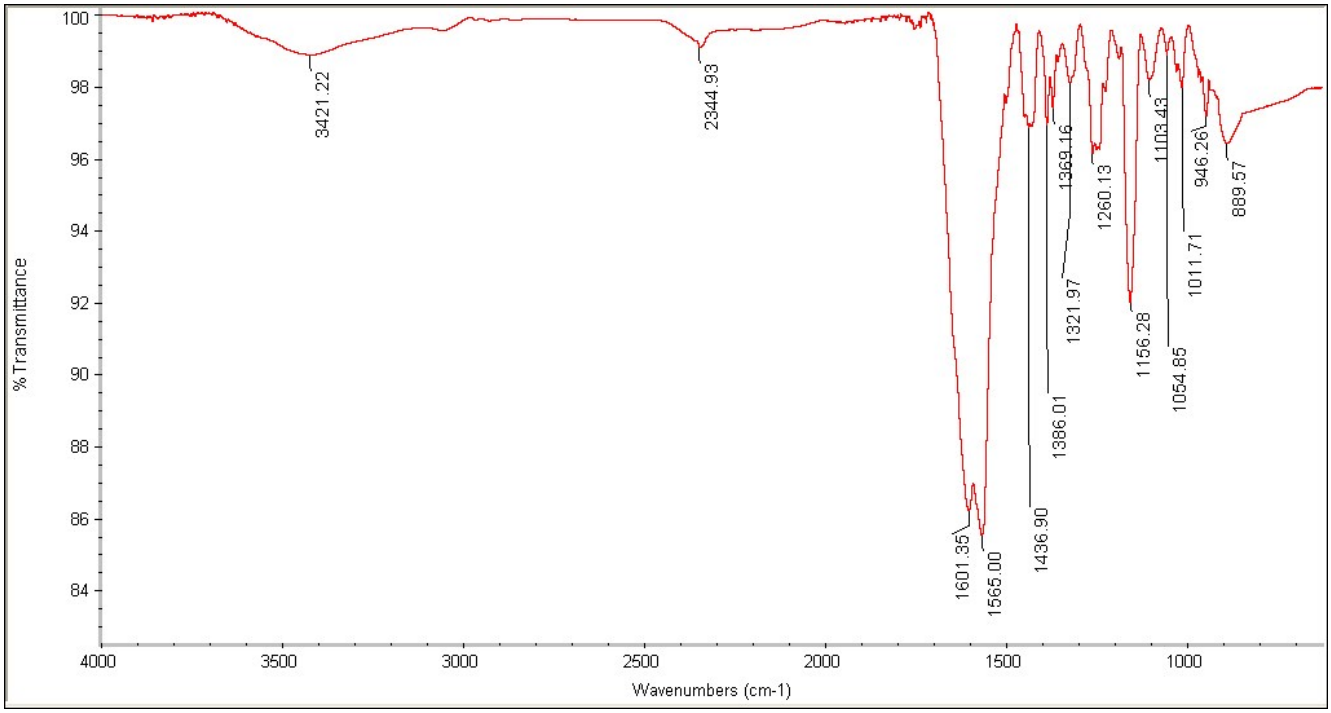

Figure. S2 The IR spectrum of complex 1

Table S1 Optimised structural parameters and Mulliken analysis for complex **1.**

State	X-ray	Doublet
Energy (eV)		**(-245554.4863)**
Selected Bond Distance (Å)		
Ni(1)-Ni(2)	2.403(2)	2.412
Ni(2)-Ni(3)	2.377(2)	2.388
Ni(1)-N(1)	2.138(6)	2.107
Ni(1)-N(4)	2.095(6)	2.108
Ni(2)-N(2)	2.047(5)	2.077
Ni(2)-N(5)	2.045(5)	2.077
Ni(3)-N(3)	2.072(6)	2.109
N(3)-N(6)	2.107(6)	2.112
Ni(1)-Cl	2.328(3)	2.342
Ni(3)-Cl	2.342(3)	2.356
Γ torsion angle (°)	(N1-Ni1-Ni2-N2) 19.97	18.48
	(N4-Ni1-Ni2-N5) 20.05	18.49
	(N2-Ni2-Ni3-N3) 22.73	18.95
	(N5-Ni2-Ni3-N6) 21.29	18.96

Mulliken Analysis	S=1/2
Atom	spin density
Ni(1)	-1.27
Ni(2)	0.81
Ni(3)	1.23

All the DFT calculations are carried out with ORCA 3.0.3[1] and the BP86 exchange-correlation functional[2-4], which had quite a good performance in these EMCAs (Extended metal-atom chain) molecules on geometries and electronic structures[5-6]. The def2-SVP basis set[7] and def2-SVP/J auxiliary basis set[8,9] are used for H and C atoms. For N, S atom, def2-TZVP(-f) basis set[10] and def2-TZVP/J auxiliary basis set[8,9] are used. And as for transition metal atoms, def2-TZVPP basis set[10] and def2-TZVPP/J auxiliary basis set[8,9] is chosen.

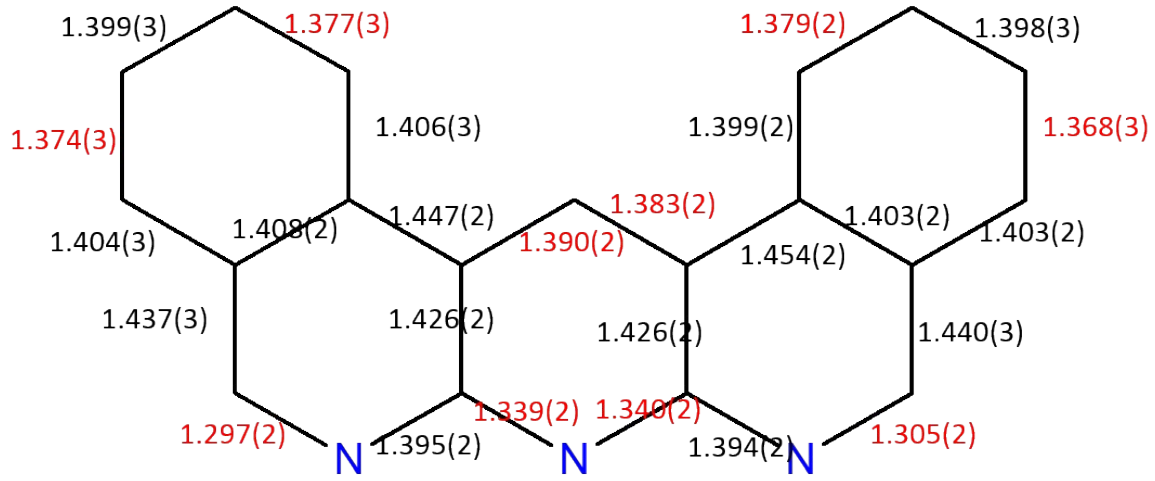

(a)

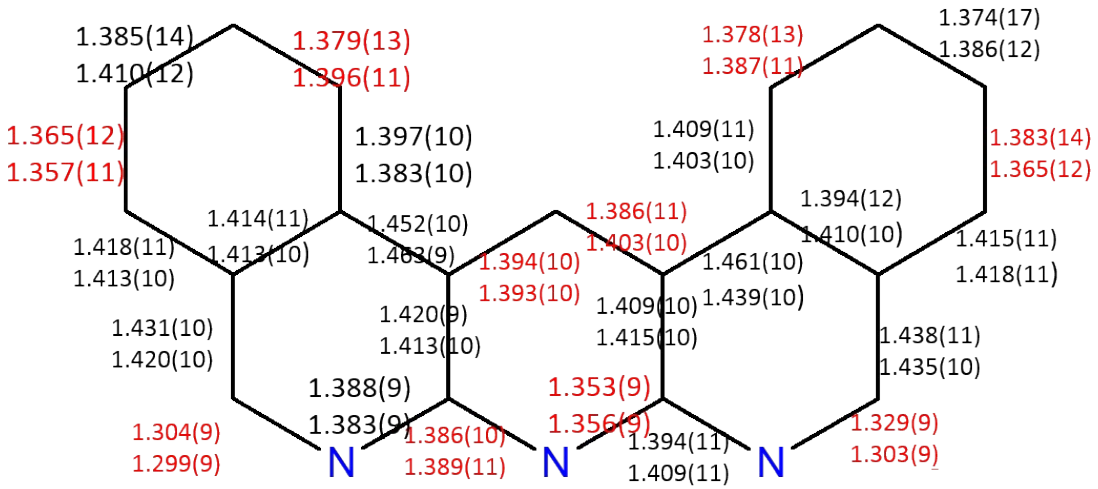

(b)

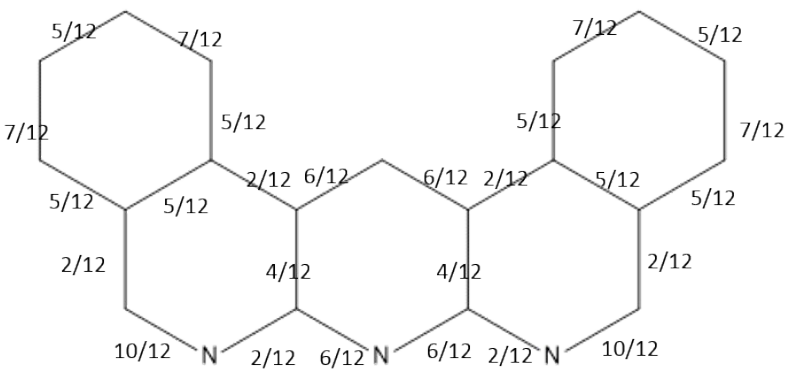

(c)

Figure. S3 (a) bond lengths (Å) of dbay ligand (b) complex 1 and (c) π bond order of C-C and C-N bonds in dbay ligands

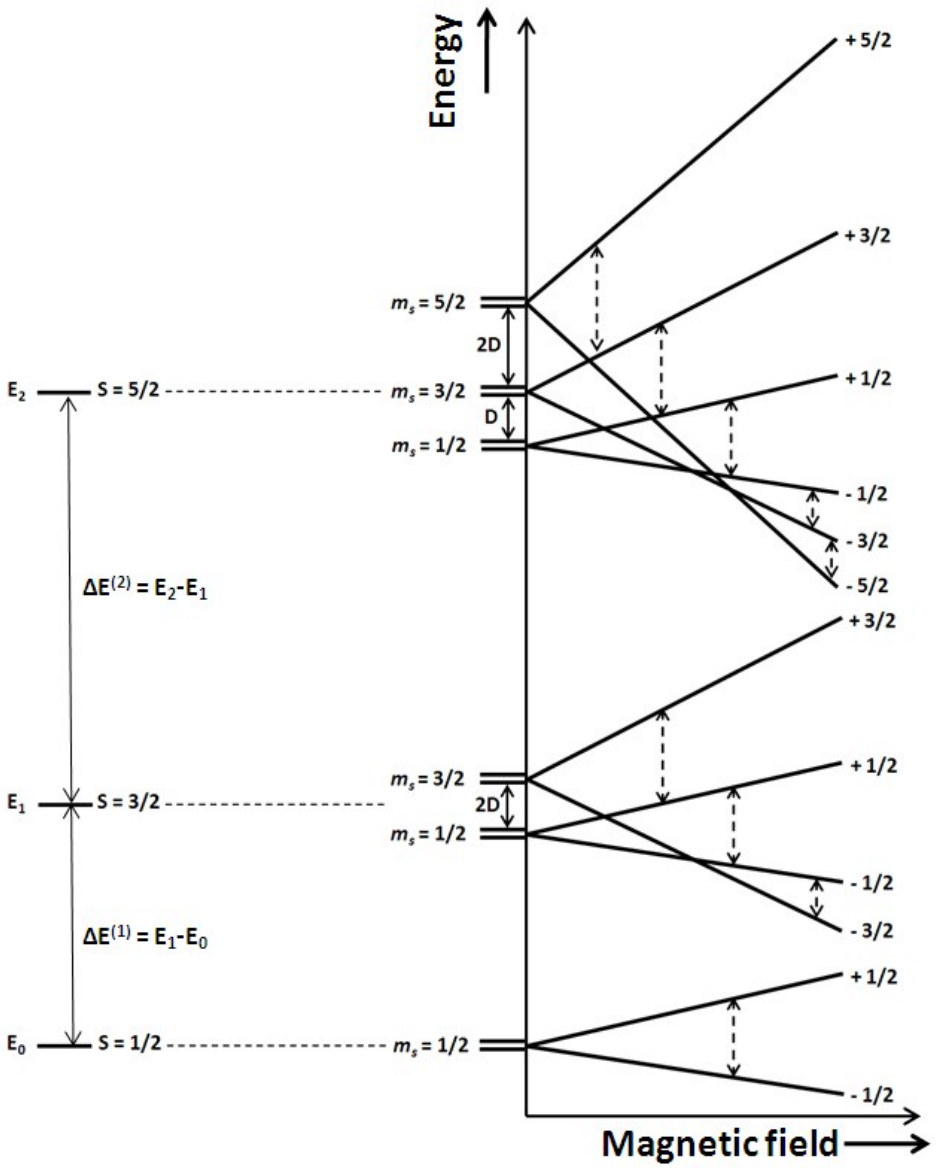

Figure S4**.** Zeeman energy diagram of coupled three-spin magnetic centers. The couplings of $S_A = 1$ and $S_B = 3/2$ would give rise to three spin states (in bold face font): **S** =1/2, 3/2 and 5/2. The spin states of 3/2 and 5/2 further consist of Kramers' doublets as shown in the diagram.

Table S2 Best fit EPR parameters of $[Ni_3(dbay)_4Cl_2]I_3$ complex at 25K.

Parameters	S_1 **= 1/2**	S_2 **= 3/2**	S_3 **= 5/2**
g_{eff}-values	2.01[a], 2.01, 2.23	2.12[a],	2.15
g-Strain(broadening)	0.03	0.08	9.95
[D,E], cm^{-1}	–	0.834, -0.0067	0.007
Linewidth, mT	3	7	5
Weighing factor	70%	29.9%	0.1%
^{14}N splitting, MHz	28, 30, 28, 28		

* Note: (a) The g = 2.01 corresponding the transition from ms=-½ to ms= +½, which could arise from S = 1/2, 3/2, and 5/2 spin states. The overall average g value easured in EPR is 2.09 in comparison to 2.12 obtained in SQUID measurement. (b) The population weighing factor is calculated by (individual weight/ total weight)x*100%; individual weight: integrated intensity assumed in the simulation for three spin states, total weight: sum of three spin state weights.

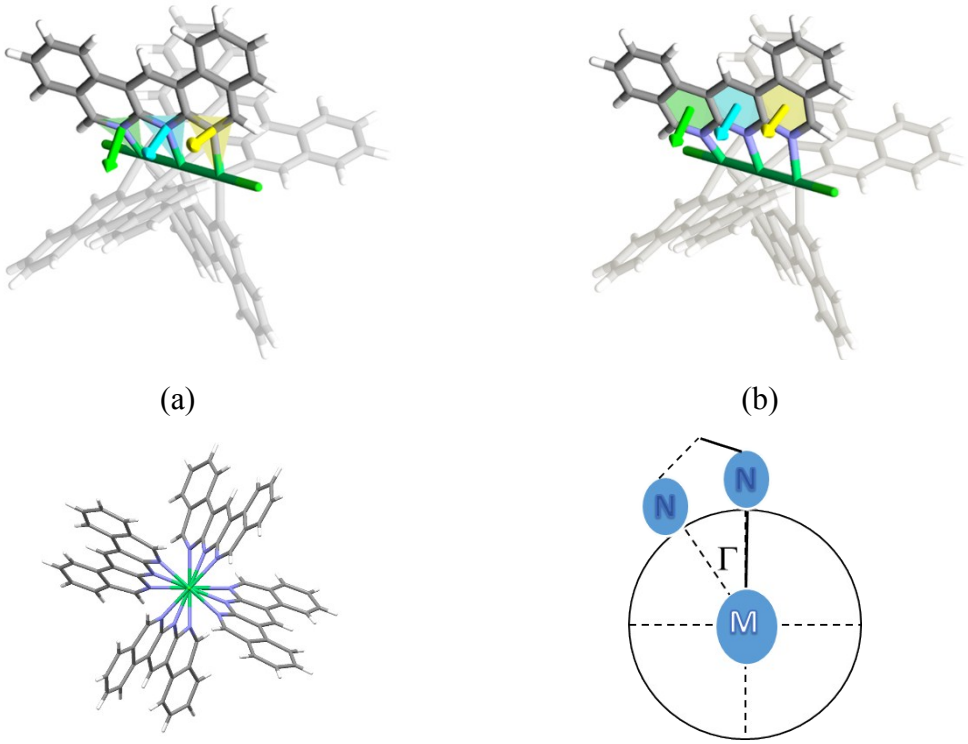

Figure S5. Arrows in (a) and (b) indicate the normal vectors of surfaces filled with the same colours as the arrow. And the twist angles of pyridyl rings: Φ (°) are defined by the angles of two neighbour normal vectors. Φ_N and Φ_{py} represent the average twist angel located on nitrogen atoms and the center of pyridyl rings. (c) and (d) Illustration of Torsion angle ∠N-M-M-N : Γ (°) viewed along the z-axis.

Table S3 Comparison two angles between complex **1** and $Ni_3(dpa)_4Cl_2$

	Average torsion angle : Γ (°)	Average twist angle : Φ_N (°)	Average twist angle : Φ_{py} (°)
1	20.5	16.67	5.83
$Ni_3(dpa)_4Cl_2$	22.5	27.09	43.24

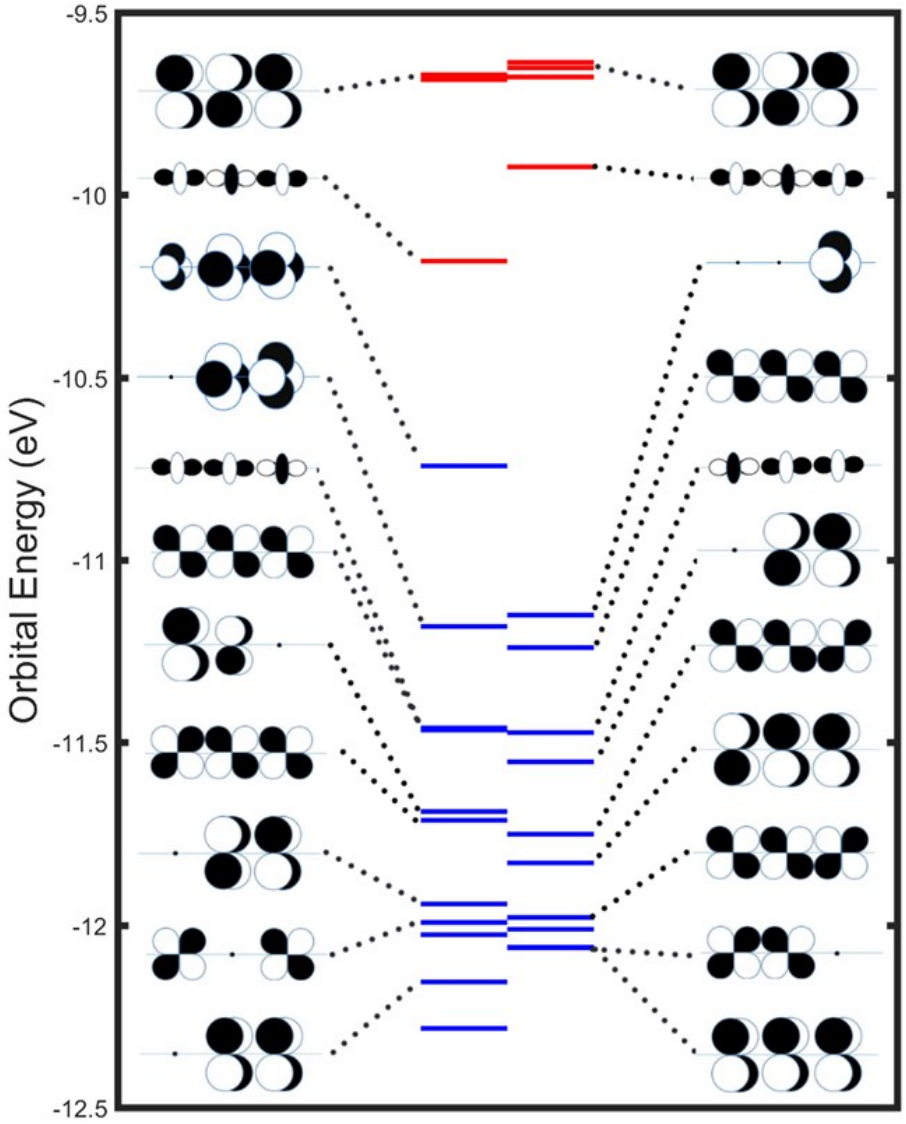

Figure S6 Occupied orbitals near the HOMO of $[Ni_3(dbay)_4Cl_2]^{3+}$.

Figure S6 is the orbital diagram of $[Ni_3(dbay)_4Cl_2]^{3+}$, and the blue line and red lines represent the occupied and unoccupied orbitals separately. The HOMO of $[Ni_3(dbay)_4Cl_2]^{3+}$ is mainly constructed from dx^2-y^2 orbitals of the Ni(2) and Ni(3) which is consistent with the experimental observation of asymmetric nickel chain and shorter Ni(2)-Ni(3) bond. Furthermore, this nonbonding δ type HOMO also has M-N antibonding character, which agrees with the elongated Ni(2)-N_{av} distances from X-ray. The DFT calculations of one-electron oxidation state $[Ni_3(dbay)_4Cl_2]^{4+}$ further verified the previous assumptions. After removing the electron from HOMO of $[Ni_3(dbay)_4Cl_2]^{4+}$ become a C_2 symmetrical central nickel chain (Ni-Ni = 2.417 Å), and Ni-N bonds are also shortened with Ni(2)-N_{av} changing from 2.077 to 1.996 Å(±0.117), and Ni(3) -N_{av} from 2.109 to 2.069 Å(±0.04).

Table S4 Optimized Cartesian Coordinates

XYZ file generated by orca_plot on BaseName=Ni3_S12

Ni	13.330112	4.632753	34.032489
Ni	13.330111	4.632747	31.620207
Ni	13.330265	4.632914	29.232297
Cl	13.330261	4.632716	36.374327
Cl	13.330244	4.632727	26.876118
N	11.822392	6.095963	33.856113
N	11.450491	5.516874	31.631698
N	11.242249	4.878291	29.402825
N	14.792385	6.139172	33.857504
N	14.214235	6.512323	31.633001
N	13.575584	6.722974	29.404515
C	11.490547	6.809654	34.922154
H	12.176748	6.723825	35.780903
C	10.308841	7.607260	35.036574
C	10.041536	8.344259	36.222982
H	10.768053	8.320716	37.050356
C	8.863614	9.079568	36.331839
H	8.648009	9.650751	37.246969
C	7.937113	9.086475	35.260683
H	7.006956	9.667931	35.351289
C	8.184497	8.365665	34.088344
H	7.442632	8.400578	33.277429
C	9.375157	7.612657	33.950416
C	9.735632	6.840280	32.768172
C	10.997967	6.149323	32.741895
C	8.914185	6.714433	31.635141
H	7.921426	7.182841	31.635546
C	9.337762	6.004749	30.499535
C	10.673942	5.469488	30.520857
C	8.512701	5.801248	29.315690
C	7.172064	6.235861	29.184301
H	6.669793	6.769499	30.004121
C	6.460958	5.981625	28.007495
H	5.418626	6.323678	27.921306
C	7.060787	5.290834	26.926223
H	6.483642	5.103066	26.008539

C	8.379649	4.854973	27.029229
H	8.863304	4.324340	26.194648
C	9.115722	5.102562	28.220268
C	10.483367	4.697906	28.331444
H	10.988227	4.236580	27.466830
C	15.506902	6.469643	34.923523
H	15.419855	5.783457	35.782145
C	16.306242	7.650085	35.038140
C	17.043848	7.916023	36.224484
H	17.019468	7.189222	37.051604
C	17.780514	9.093031	36.333804
H	18.351951	9.307627	37.249020
C	17.788306	10.020034	35.263071
H	18.370796	10.949523	35.354009
C	17.066950	9.774035	34.090784
H	17.102595	10.516172	33.280141
C	16.312502	8.584322	33.952486
C	15.539398	8.225430	32.770285
C	14.847051	6.963814	32.743461
C	15.414612	9.047513	31.637576
H	15.884473	10.039601	31.638289
C	14.704096	8.625435	30.501983
C	14.167494	7.289772	30.522682
C	14.501751	9.451079	29.318333
C	14.937439	10.791456	29.187697
H	15.470481	11.293119	30.008272
C	14.684655	11.503122	28.010915
H	15.027437	12.545267	27.925415
C	13.994371	10.904147	26.928856
H	13.807800	11.481688	26.011173
C	13.557214	9.585651	27.031167
H	13.026398	9.102841	26.196227
C	13.803253	8.849052	28.222189
C	13.396757	7.481914	28.333042
H	12.935333	6.977693	27.468103
N	14.837902	3.169556	33.856025
N	15.209843	3.748772	31.631642
N	15.418143	4.387435	29.402802

N	11.867892	3.126495	33.857601
N	12.446053	2.753311	31.633107
N	13.084775	2.542618	29.404646
C	15.169714	2.455793	34.922027
H	14.483474	2.541534	35.780751
C	16.351432	1.658206	35.036443
C	16.618720	0.921152	36.222821
H	15.892168	0.944616	37.050167
C	17.796671	0.185893	36.331690
H	18.012260	-0.385332	37.246798
C	18.723218	0.179087	35.260573
H	19.653399	-0.402331	35.351187
C	18.475848	0.899945	34.088262
H	19.217749	0.865116	33.277376
C	17.285156	1.652904	33.950322
C	16.924688	2.425313	32.768097
C	15.662352	3.116271	32.741825
C	17.746151	2.551185	31.635082
H	18.738906	2.082770	31.635484
C	17.322593	3.260902	30.499492
C	15.986424	3.796184	30.520820
C	18.147673	3.464433	29.315665
C	19.488295	3.029776	29.184267
H	19.990529	2.496058	30.004059
C	20.199430	3.284062	28.007489
H	21.241748	2.941974	27.921294
C	19.599643	3.974948	26.926254
H	20.176810	4.162755	26.008592
C	18.280795	4.410847	27.029266
H	17.797175	4.941548	26.194709
C	17.544693	4.163208	28.220277
C	16.177057	4.567883	28.331450
H	15.672248	5.029289	27.466854
C	11.153341	2.796072	34.923614
H	11.240412	3.482252	35.782236
C	10.353937	1.615674	35.038225
C	9.616314	1.349769	36.224566
H	9.640727	2.076566	37.051688

C	8.879594	0.172796	36.333884
H	8.308146	-0.041776	37.249098
C	8.871761	-0.754206	35.263150
H	8.289230	-1.683669	35.354086
C	9.593129	-0.508238	34.090864
H	9.557455	-1.250376	33.280223
C	10.347634	0.681439	33.952568
C	11.120756	1.040291	32.770367
C	11.813183	2.301855	32.743554
C	11.245491	0.218208	31.637649
H	10.775562	-0.773847	31.638350
C	11.956054	0.640242	30.502070
C	12.492767	1.975863	30.522777
C	12.158360	-0.185412	29.318420
C	11.722544	-1.525744	29.187756
H	11.189403	-2.027353	30.008300
C	11.975314	-2.237432	28.010985
H	11.632431	-3.279541	27.925463
C	12.665721	-1.638524	26.928968
H	12.852282	-2.216078	26.011291
C	13.103007	-0.320072	27.031309
H	13.633912	0.162690	26.196397
C	12.856975	0.416550	28.222317
C	13.263598	1.783650	28.333191
H	13.725108	2.287828	27.468275

References:

1. Neese, F. The ORCA program system. *Wiley Interdiscip. Rev. Comput Mol. Sci.* **2012**, *2*, 73-78
2. Perdew, J. P. Density-functional approximation for the correlation energy of the inhomogeneous electron gas. *Phys. Rev. B* **1986**, *33*, 8822.
3. Perdew, J. P. Erratum: Density-functional approximation for the correlation energy of the inhomogeneous electron gas. *Phys. Rev. B* **1986**, *34*, 7406.
4. Becke, A. D. Density-functional exchange-energy approximation with correct asymptotic behavior. *Phys. Rev. A* **1988**, *38*, 3098.
5. Brogden, D. W.; Berry, J. F. Heterometallic Multiple Bonding: Delocalized Three-Center σand π Bonding in Chains of 4d and 5d Transition Metals. *Inorg. Chem.* **2014**, *53*, 11354-11356
6. Brogden, D. W.; Berry, J. F. Heterometallic Second-Row Transition Metal Chain Compounds in Two Charge States: Syntheses, Properties, and Electronic Structures of [Mo-Mo-Ru]$^{6+/7+}$ Chains. *Inorg. Chem.* **2015**, *54*, 7660-7665.
7. Schäfer, A.; Horn, H.; Ahlrichs, R. Fully optimized contracted Gaussian basis sets for atoms Li to Kr. *J. Chem. Phys*. **1992**, *97*, 2571-2577.
8. Eichkorn, K.; Treutler, O.; Öhm, H.; Häser, M.; Ahlrichs, R. Auxiliary basis sets to approximate Coulomb potentials. *Chem. Phys. Lett.* **1995**, *240*, 283-290.
9. Eichkorn, K.; Weigend, F.; Treutler, O.; Ahlrichs, R. Auxiliary basis sets for main row atoms and transition metals and their use to approximate Coulomb potentials. *Theor. Chem. Acc*. **1997**, *97*, 119-124.
10. Weigend, F.; Ahlrichs, R. Balanced basis sets of split valence, triple zeta valence and quadruple zeta valence quality for H to Rn: Design and assessment of accuracy. *Phys. Chem. Chem. Phys*. **2005**, *7*, 3297-3305.